We are IntechOpen, the world's leading publisher of Open Access books Built by scientists, for scientists

4,800
Open access books available

122,000
International authors and editors

135M
Downloads

Our authors are among the

154
Countries delivered to

TOP 1%
most cited scientists

12.2%
Contributors from top 500 universities

CLARIVATE ANALYTICS BOOK CITATION INDEX INDEXED

WEB OF SCIENCE™

Selection of our books indexed in the Book Citation Index in Web of Science™ Core Collection (BKCI)

Interested in publishing with us?
Contact book.department@intechopen.com

Numbers displayed above are based on latest data collected.
For more information visit www.intechopen.com

Chapter 5

Organization of Two Cortico–Basal Ganglia Loop Circuits That Arise from Distinct Sectors of the Monkey Dorsal Premotor Cortex

Masahiko Takada, Eiji Hoshi, Yosuke Saga, Ken-ichi Inoue, Shigehiro Miyachi, Nobuhiko Hatanaka, Masahiko Inase and Atsushi Nambu

Additional information is available at the end of the chapter

http://dx.doi.org/10.5772/54822

1. Introduction

The importance of loop circuits linking the frontal cortex and the basal ganglia has constantly been highlighted in the performance of various motor schemes [1-4]. These cortico–basal ganglia loop circuits originate from anatomically and functionally diverse motor-related areas, which include the primary motor cortex (MI), the supplementary motor area (SMA), and the premotor cortex (PM). Two opposing mechanisms are possible for the processing of motor information in the cortico–basal ganglia loops. One is "information funneling" in which inputs from multiple motor-related areas are highly concentrated in common territories of the basal ganglia. The other is "parallel processing" in which inputs from distinct motor-related areas are topographically distributed to individual territories of the basal ganglia. For understanding the mode of motor information processing in the basal ganglia, it is crucial to investigate which mechanism organizes the projections from the frontal motor-related areas to the input stations of the basal ganglia, the striatum and the subthalamic nucleus (STN).

According to several physiological studies [5-8], it has been revealed that the caudal aspect of the dorsal premotor cortex (F2; see [9,10]) in area 6 of macaque monkeys plays a crucial role in the planning and execution of arm movements, and that there is certain functional specialization between the caudal sector of F2 (F2c), located ventral to the superior precentral dimple, and the rostral sector of F2 (F2r), located dorsal to the genu of the arcuate sulcus. Since our prior work demonstrates that F2c and F2r receive largely segregated inputs from the cerebellum [11], it is of great interest to explore the organization of cortico–basal ganglia loop circuits that arise from F2c and F2r.

In this chapter, we first summarize a series of our previous anatomical studies about the mode of information processing in the basal ganglia based on the distribution patterns of corticostriatal and corticosubthalamic inputs from the frontal motor-related areas of macaque monkeys, including the PM [12-18]. The overall results indicate that the corticostriatal and corticosubthalamic inputs from the motor-related areas are orderly arranged according to segregation versus overlap rules. We then introduce the data of our recent work concerning the organization of multisynaptic pathways that connect the basal ganglia with F2. In this study, we investigated the distributions of cells of origin in the basal ganglia of multisynaptic inputs to F2c and F2r [19]. Employing retrograde transsynaptic transport of rabies virus, we have demonstrated that neuronal populations giving rise to the projections to F2c and F2r are substantially segregated in the internal segment of the globus pallidus (GPi) and the substantia nigra pars reticulata (SNr) (i.e., the output stations of the basal ganglia), whereas intermingling rather than segregation governs for the other basal ganglia components, involving the external segment of the globus pallidus (GPe), STN, and the striatum (i.e., the input stations of the basal ganglia). This suggests that the loop circuits linking F2 and the basal ganglia may possess a common convergent window at the input stage and constitute parallel divergent channels at the output stage. The major part the present experiments was carried out at the Tokyo Metropolitan Institute for Neuroscience, Tokyo Metropolitan Organization for Medical Research. The experimental protocol was approved by the Animal Care and Use Committee of the Tokyo Metropolitan Institute for Neuroscience, and all experiments were conducted in accordance with the Guidelines for the Care and Use of Animals (Tokyo Metropolitan Institute for Neuroscience, 2000).

2. Organization of corticostriatal and corticosubthalamic inputs

In a series of our previous anatomical studies, we have analyzed the distribution patterns of corticostriatal and corticosubthalamic inputs from the frontal motor-related areas of macaque monkeys [12-18]. The frontal motor-related areas that we have examined widely include the MI, SMA, dorsal and ventral divisions of the PM (PMd and PMv), presupplementary motor area (pre-SMA), and rostral and caudal divisions of the cingulate motor area (CMAr and CMAc). In our studies, we initially performed intracortical microstimulation to map these areas. Then, different anterograde tracers were injected separately into somatotopically corresponding regions of given areas; the forelimb regions were tested except for the MI and SMA). The overall results indicate that corticostriatal and corticosubthalamic input zones from the frontal motor-related areas are orderly distributed in a topographical fashion, but display complex patterns of segregation versus overlap of one another (Figs. 1, 2).

With respect to the corticostriatal inputs from the MI and SMA, dense input zones from the MI are located predominantly in the lateral aspect of the caudal putamen, whereas those from the SMA are in the medial aspect. On the other hand, corticostriatal inputs from the PMd and PMv are distributed mainly in the dorsomedial sector of the putamen, although these two input zones are virtually devoid of overlap. Thus, the corticostriatal input zones from the MI and SMA were considerably segregated though partly overlapped in the mediolateral central aspect of the putamen, while the corticostriatal input zones from the

PMd and PMv largely overlap that from the SMA, but not from the MI (Fig. 1; see also [14,15]). In addition, the corticostriatal input zone from the pre-SMA is located primarily in the striatal cell bridges and their neighboring regions of the caudate nucleus and the putamen, thus indicating that the corticostriatal input from the pre-SMA is spatially separate from those from the MI, SMA, and PMd/PMv (Fig. 1; see also [17]). As for the CMAr and CMAc, corticostriatal inputs from the CMAr and CMAc are located within the rostral striatum, with the highest density in the striatal cell bridge region or the ventrolateral portion of the putamen, respectively. There is no substantial overlap between these input zones. The corticostriatal input zone from the CMAr considerably overlaps that from the pre-SMA, while the input zone from the CMAc displays a large overlap with that from the MI (Fig. 1; see also [16]). Moreover, it has also shown that the rostral aspect of the PMd (F7; see [9,10]) projects predominantly to the striatal cell bridge region [18].

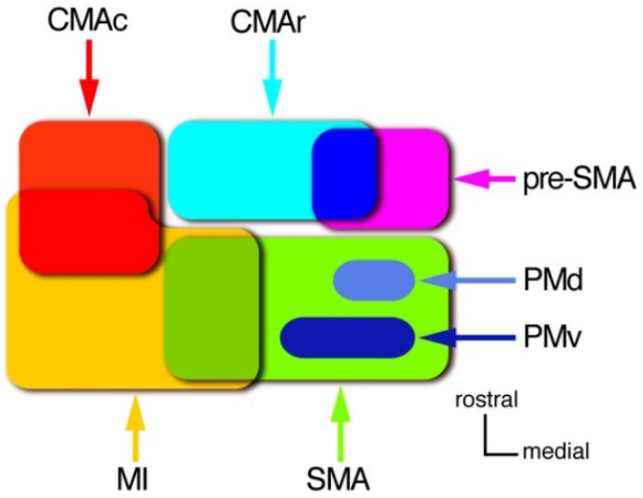

Figure 1. Summary diagram showing the organization of corticostriatal input zones in the putamen that arise from the frontal motor-related areas. These input zones are orderly distributed in a topographical fashion, but display complex patterns of segregation and overlap.

The overall pattern of corticosubthalamic input distributions is essentially the same as that of corticostriatal input distributions. The corticosubthalamic input zones from the MI and CMAc are located mainly within the lateral aspect of the STN, thereby leading to a large overlap of the two input zones. On the other hand, the major input zones from the SMA, pre-SMA, PMd, PMv, and CMAr within the medial aspect of the STN where a varying degree of overlaps are apparent between the input zones (Fig. 2; see also [12,13,16,17].

In terms of the somatotopical representation, the corticostriatal input zones from regions of the frontal motor-related areas (i.e., the MI, SMA, and PM) representing the hindlimb, forelimb, and orofacial part are, in this order, arranged from dorsal to ventral within the putamen (Fig. 3; see also [14]). A similar pattern is most likely to organize the somatotopical arrangement of cortical motor inputs within the GPe and GPi (Fig. 3). Of particular interest is that dual sets of body part representations underlie the somatotopical arrangement in the STN. Somatotopical representations in the lateral part of the STN are arranged from medial to lateral in the order of the hindlimb, forelimb, and orofacial part. By contrast, these body parts in the medial

counterpart are represented mediolaterally in the inverse order, as though reflecting a "mirror image" against the somatotopical arrangement in the lateral STN (Fig. 3; see also [12]).

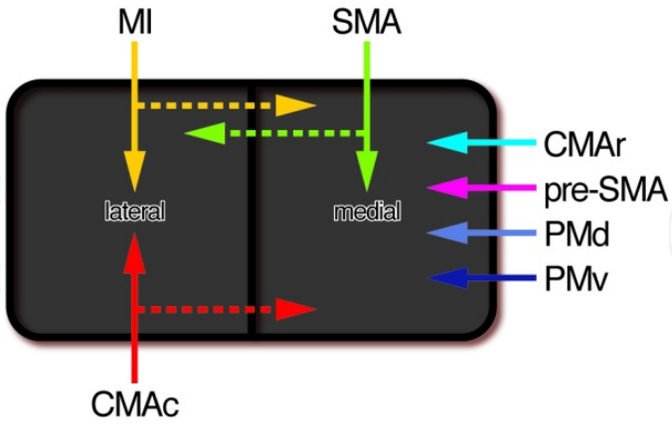

Figure 2. Summary diagram showing the organization of corticosubthalamic input zones from the frontal motor-related areas. Broken arrows represent minor projections.

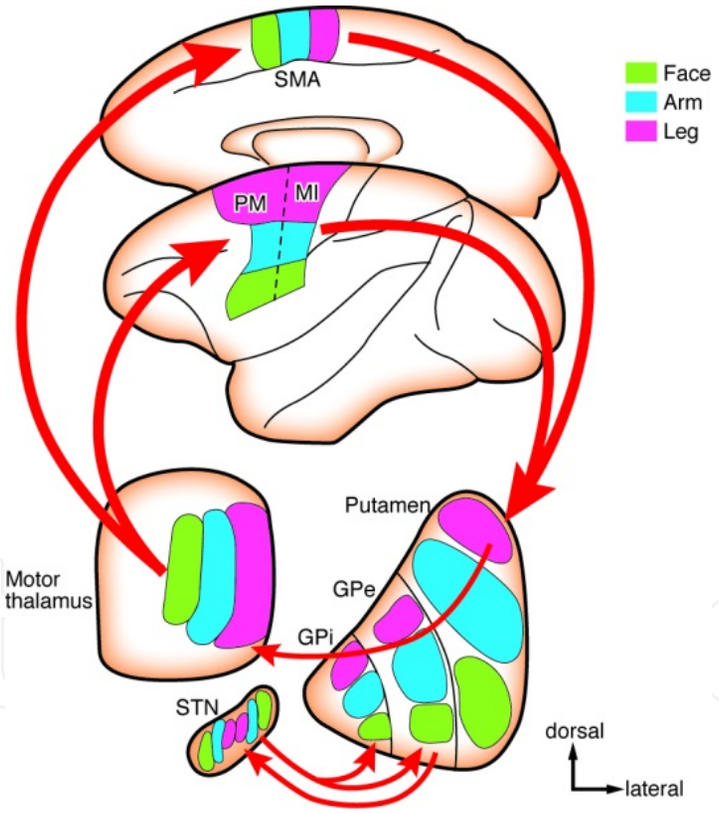

Figure 3. Cortico–basal ganglia loop circuits arising from the frontal motor-related areas (i.e., the MI, SMA, and PM) in terms of the somatotopical representation. Corticostriatal input zones from regions of representing the hindlimb, forelimb, and orofacial part are, in this order, arranged from dorsal to ventral within the putamen and GPe/GPi. In the STN, there exist dual sets of body part representations. Somatotopical representations in the lateral STN are arranged from medial to lateral in the order of the hindlimb, forelimb, and orofacial part, whereas the medial STN exhibits a mediolaterally reversed pattern of the representations, thereby reflecting a "mirror image" against the somatotopical arrangement in the lateral STN.

3. Organization of multisynaptic pathways linking F2 and the basal ganglia

3.1. Rabies injections

Multiple injections of rabies virus were made into F2c and F2r in the PMd (Fig. 4). The injection sites were determined according to the results of our previous electrophysiological work in which we demonstrated that the neuronal response properties involved in planning and executing reaching movements differed in F2r and F2c [20]. This rostrocaudal segregation is consistent with the classification schema that emerged in previous studies [10,21,22]. The rabies injections were carried out lateral to the superior precentral dimple for the F2c procedure (Fig. 4B). For the F2r procedure, on the other hand, the rabies injections were done around the genu of the arcuate sulcus (Fig. 4C).

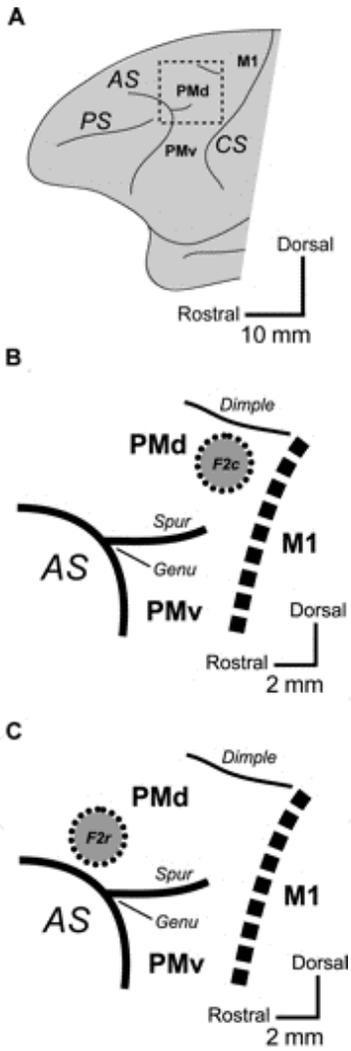

Figure 4. Locations of the injection sites in F2c and F2r. (A) Diagram illustrating the macaque lateral frontal lobe. The rectangular area drawn with broken lines in (A) is enlarged in (B) and (C). (B,C) Injection sites of rabies virus in F2c (B) and F2r (C). In (B) and (C), the border between the PMd/PMv and the MI is represented with the broken line. AS, arcuate sulcus; CS, central sulcus; Dimple, superior precentral dimple; Genu, genu of the AS; PS, principal sulcus; Spur, spur of the AS.

3.2. Origins of basal ganglia inputs to F2c and F2r

Three days after the rabies injection into F2c or F2r, a number of labeled neurons were observed in the GPi and SNr. These neurons are considered to send outputs to F2c or F2r via the ventral nuclei or mediodorsal nucleus of the thalamus. No labeled neurons were found in the GPe at this stage, indicating that only the second-order neuron labeling occurred at the 3-day postinjection period.

The distribution of labeled neurons observed in the GPi after the F2c injection differed from that observed after the F2r injection (Fig. 5). Two-dimensional density maps of the GPi were prepared to separately represent the labeling patterns in outer and inner portions (Fig. 5A). These maps showed that the distributions of GPi neurons projecting to F2c and F2r were segregated in both portions, each of which received input from the striatum [23]. After the F2c injection, the labeled neurons were distributed broadly in the ventral part of the GPi at its caudal level (Fig. 5B). By contrast, the labeled neurons after the F2r injection were located in the dorsal part of the GPi at its rostocaudal middle level (Fig. 5C).

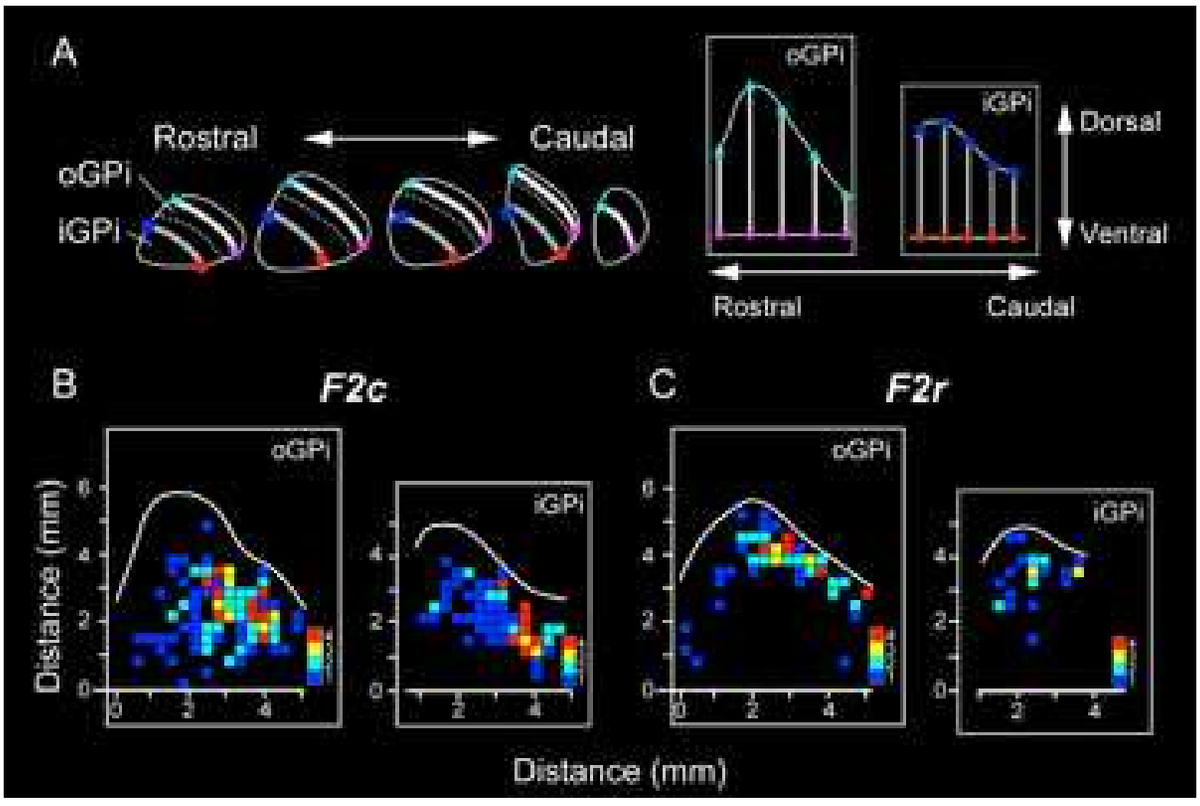

Figure 5. Density maps of GPi neuron labeling after rabies injections into F2c and F2r. (A) Procedures to construct two-dimensional density maps of the GPi. The unfolding process started with drawing lines through the center of the outer (oGPi) and inner (iGPi) portions of the GPi (left). The reference points were placed at the bottom (specified by pink stars or red circles) and the top (specified by cyan triangles or blue squares) of the GPi. The position of each labeled neuron was projected onto the central line. Then, each line through the nucleus was aligned on the ventral edge of the GPi (right). The GPi was divided into 300 μm x 300 μm bins. (B) Density maps of oGPi and iGPi neuron labeling after F2c injection. (C) Density maps of oGPi and iGPi neuron labeling after F2r injection. The number of labeled neurons in each bin was counted and color-coded.

The rabies injections into F2c and F2r resulted in different distributions of neuronal labeling in the SNr. After the F2c injection, labeled neurons in the SNr were found in the central part through the caudal half of the SNr. After the F2r injection, on the other hand, labeled neurons were distributed primarily throughout the rostral half of the SNr (data not shown).

By extending the postinjection period to 4 days, we detected neuronal labeling in the GPe, STN, and striatum. In the GPe, labeled neurons were widely distributed over the nucleus following the F2c injection, whereas they occupied a more restricted area following the F2r injection (Fig. 6). To compare the two distribution patterns in detail, two-dimensional density maps of the GPe were prepared to depict the results from the F2c and F2r injections (Fig. 6A). In the F2r injection case, the labeled neurons were located only in the rostral and dorsal portions of the GPe (Fig. 6C), while those in the F2c injection case were found not only in the rostral and dorsal portions, but also in the caudal and ventral portions of the GPe (Fig. 6B). These data indicated that the area in which GPe neurons projected trisynaptically to F2r was included within the area in which GPe neurons projected to F2c.

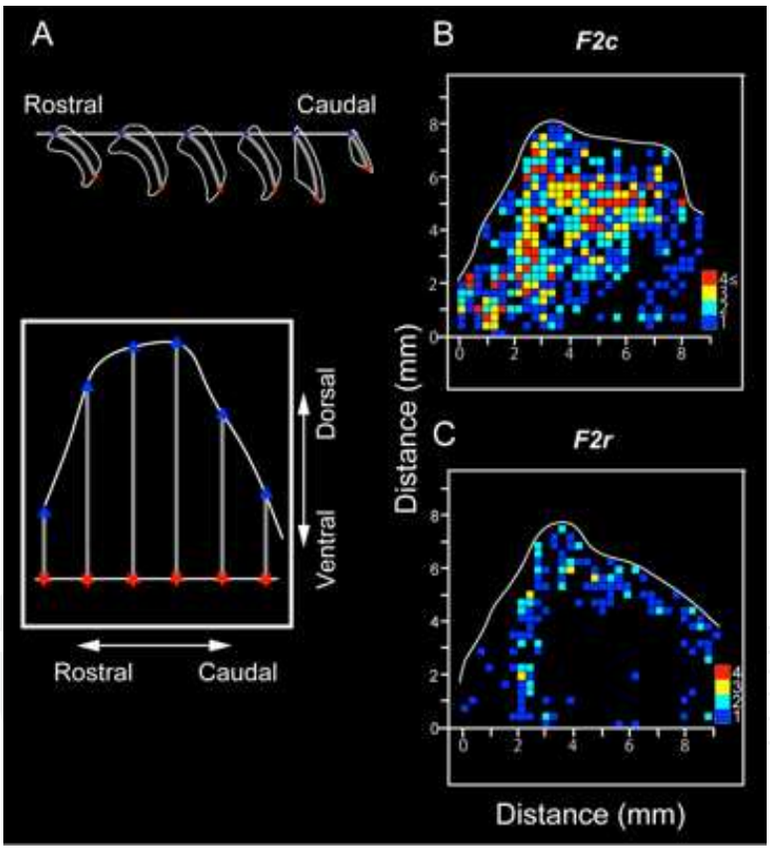

Figure 6. Density maps of GPe neuron labeling after rabies injections into F2c and F2r. (A) Procedures to construct two-dimensional density maps of the GPe. The unfolding process started with drawing lines through the center of the GPe (top). The reference points were placed at the bottom (specified by red stars) and the top (specified by blue triangles) of the GPe. The position of each labeled neuron was projected onto the central line. Then, each line through the nucleus was aligned on the ventral edge of the GPe (bottom). The GPe was divided into 300 μm x 300 μm bins. (B) Density map of GPe neuron labeling after F2c injection. (C) Density map of GPe neuron labeling after F2r injection. The number of labeled neurons in each bin was counted and color-coded.

In Figure 7, density maps of neuronal labeling in the STN are shown. After the F2r injection, labeled neurons were located primarily in the ventral aspect (Fig. 7, lower row), whereas the area of rabies labeling after the F2c injection expanded more dorsally (Fig. 7, upper row).

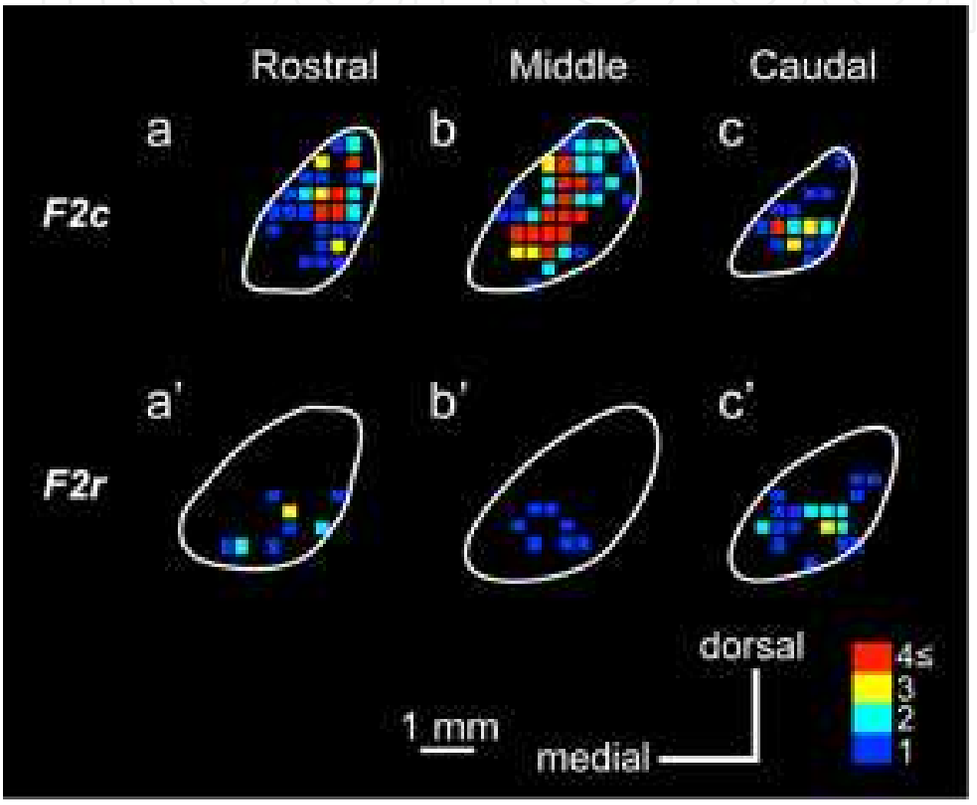

Figure 7. Distributions of STN neuron labeling after rabies injections into F2c and F2r. Three equidistant coronal sections are arranged rostrocaudally in a-c (after F2c injection) and a'-c' (after F2r injection). The STN was divided into 300 μm x 300 μm bins. The number of labeled neurons in each bin was counted and color-coded.

Large numbers of labeled neurons were observed in the striatum. Following each injection, the labeled neurons were widely distributed in the striatal cell bridges and their neighboring regions of the caudate nucleus and the putamen (Fig. 8). In addition, dense neuron labeling was seen in the ventral striatum (Fig. 8).

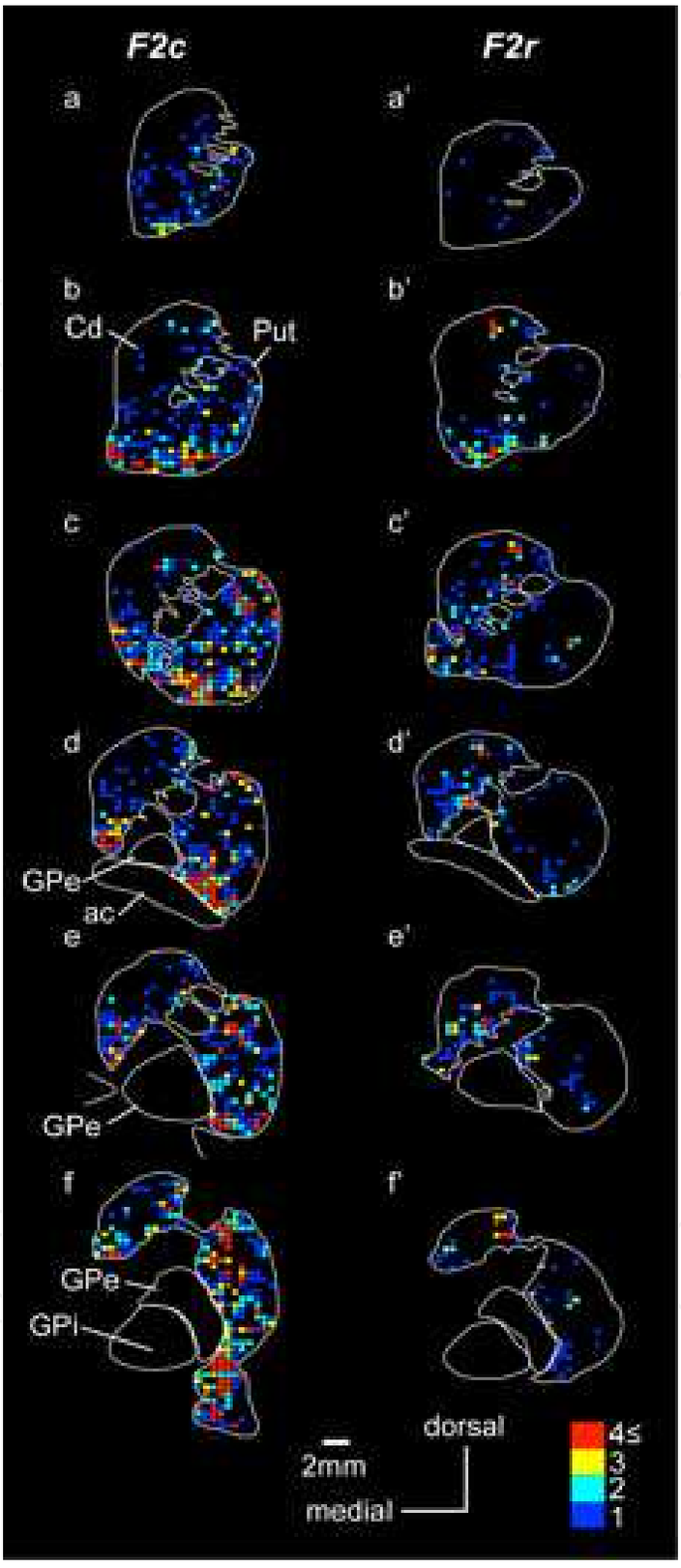

Figure 8. Distributions of striatal neuron labeling after rabies injections into F2c and F2r. Six equidistant coronal sections are arranged rostrocaudally in a-f (after F2c injection) and a'-f' (after F2r injection). The striatum was divided into 500 μm x 500 μm bins. The number of labeled neurons in each bin was counted and color-coded. ac, anterior commissure; Cd, caudate nucleus; Put, putamen.

4. Conclusion

Here, we propose that two separate channels, each of which projects multisynaptically to F2c and F2r, may be operated in the output stations of the basal ganglia (i.e., the GPi and SNr), although segregation may be obscured in the input station (i.e., the striatum) where neurons projecting multisynaptically to F2c and F2r intermingle (Fig. 9). This indicates that each of the two parallel loops (i.e., the F2c-basal ganglia loop and the F2r-basal ganglia loop)

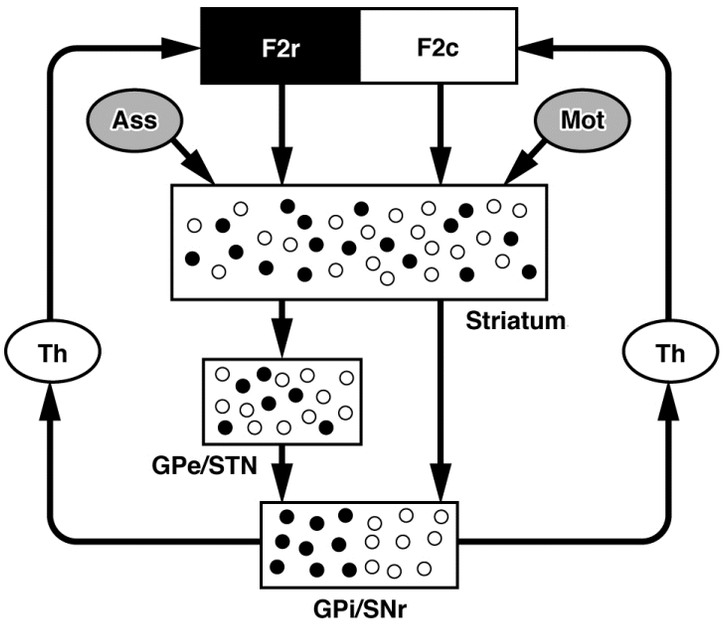

Figure 9. Schematic diagram showing the distribution patterns of cells of origin in the basal ganglia of multisynaptic inputs to F2c and F2r. In the striatum, GPe/STN, and GPi/SNr, open and filled circles indicate neurons projecting multisynaptically to F2c and F2r, respectively. In the output stations of the basal ganglia (i.e., GPi/SNr), the cells of origin of multisynaptic projections to F2c and F2r are basically segregated. On the other hand, intermingling rather than segregation is prominent for the other basal ganglia components, including the input station (i.e., striatum). Note that in the GPe/STN that connects the input and output stations, the F2r territory tends to be included within the F2c territory (see the text for detail). Ass, association cortical areas such as the prefrontal cortex; Mot, motor cortical areas such as the MI and SMA; Th, thalamus.

collects diverse inputs from the motor and association territories with which F2c and F2r are cortically interconnected. Given that individual neurons in the GPi and SNr have widespread dendritic trees [24,25], these structures may consist of zones where diverse inputs are sorted and integrated, which allows each structure to send outputs to F2c and F2r separately. On the other hand, the distribution pattern of neurons in the GPe and STN that project multisynaptically to F2c and F2r differs from that of neurons in the GPi and SNr; the F2r territory seems to be included within the F2c territory in the GPe and STN. This suggests that the mode of information processing in the GPe and STN may be distinct from that in the GPi and SNr. Together with a previous notion that there is the precise network architecture in each component of the basal ganglia [26-28], our overall results will provide a novel framework for understanding the mode of information processing in the cortico–basal ganglia loop circuits.

By analyzing the network linking F2 and the cerebellum, we have revealed that the cells of origin in the cerebellum of multisynaptic projections to F2c and F2r are segregated at the output station (i.e., the deep cerebellar nuclei), whereas both integration and segregation are evident at the input station (i.e., the cerebellar cortex) [11]. The networks connecting the basal ganglia/cerebellum with F2 may be governed by a common rule organizing the segregation at the output stage and the intermingling rather than the segregation at the input stage.

Author details

Masahiko Takada* and Ken-ichi Inoue
Systems Neuroscience Section, Primate Research Institute, Kyoto University, Inuyama, Japan

Masahiko Takada, Eiji Hoshi and Atsushi Nambu
Japan Science and Technology Agency, CREST, Tokyo, Japan

Eiji Hoshi and Yosuke Saga
Frontal Lobe Project, Tokyo Metropolitan Institute of Medical Science, Tokyo, Japan

Shigehiro Miyachi
Cognitive Neuroscience Section, Primate Research Institute, Kyoto University, Inuyama, Japan

Nobuhiko Hatanaka and Atsushi Nambu
Division of System Neurophysiology, National Institute for Physiological Sciences and Department of Physiological Sciences, Graduate University for Advanced Studies (SOKENDAI), Okazaki, Japan

* Corresponding Author

Masahiko Inase
Department of Physiology, Kinki University School of Medicine, Osaka-Sayama, Japan

5. References

[1] Alexander GE, DeLong MR, Strick PL. Parallel organization of functionally segregated circuits linking basal ganglia and cortex. Annu Rev Neurosci 1986;9: 357-381.
[2] Alexander GE, Crutcher MD. Functional architecture of basal ganglia circuits: neural substrates of parallel processing. Trends Neurosci 1990;13: 266-271.
[3] Parent A, Hazrati L-N. Functional anatomy of the basal ganglia. I. The cortico-basal ganglia-thalamo-cortical loop. Brain Res Rev 1995;20: 91-127.
[4] Mink JW. The basal ganglia: focused selection and inhibition of competing motor programs. Prog Neurobiol 1996;50: 381-425.
[5] Wise SP. The primate premotor cortex: past, present, and preparatory. Annu Rev Neurosci 1985;8:1-19.
[6] Caminiti R, Ferraina S, Mayer AB. Visuomotor transformations: early cortical mechanisms of reaching. Curr Opin Neurobiol 1998;8:753-761.
[7] Hoshi E, Tanji J. Distinctions between dorsal and ventral premotor areas: anatomical connectivity and functional properties. Curr Opin Neurobiol 2007;17:234-242.
[8] Cisek P, Kalaska JF. Neural mechanisms for interacting with a world full of action choices. Annu Rev Neurosci 2010;33:269-298.
[9] Matelli M, Luppino G, Rizzolatti G. Patterns of cytochrome oxidase activity in the frontal agranular cortex of the macaque monkey. Behav Brain Res 1985;18: 125-136.
[10] Barbas H, Pandya DN. Architecture and frontal cortical connections of the premotor cortex (area 6) in the rhesus monkey. J Comp Neurol 1987;256: 211-228.
[11] Hashimoto M, Takahara D, Hirata Y, Inoue K, Miyachi S, Nambu A, Tanji J, Takada M, Hoshi E. Motor and nonmotor projections from the cerebellum to rostrocaudally distinct sectors of the dorsal premotor cortex in macaques. Eur J Neurosci 2010;31:1402-1413.
[12] Nambu A, Takada M, Inase M, Tokuno H. Dual somatotopical representations in the primate subthalamic nucleus: evidence for ordered but reversed body-map transformations from the primary motor cortex and the supplementary motor area. J Neurosci 1996;16:2671-2683.
[13] Nambu A, Tokuno H, Inase M, Takada M. Corticosubthalamic input zones from forelimb representations of the dorsal and ventral divisions of the premotor cortex in the macaque monkey: comparison with the input zones from the primary motor cortex and the supplementary motor area. Neurosci Lett 1997;239: 13-16.
[14] Takada M, Tokuno H, Nambu A, Inase M. Corticostriatal projections from the somatic motor areas of the frontal cortex in the macaque monkey: segregation versus overlap of

input zones from the primary motor cortex, the supplementary motor area, and the premotor cortex. Exp Brain Res 1998;120: 114-128.

[15] Takada M, Tokuno H, Nambu A, Inase M. Corticostriatal input zones from the supplementary motor area overlap those from the contra- rather than ipsilateral primary motor cortex. Brain Res 1998;791: 335-340.

[16] Takada M, Tokuno H, Hamada I, Inase M, Ito Y, Imanishi M, Hasegawa N, Akazawa T, Hatanaka N, Nambu A. Organization of inputs from cingulate motor areas to basal ganglia in macaque monkey. Eur J Neurosci 2001;14:1633-1650.

[17] Inase M, Tokuno H, Nambu A, Akazawa T, Takada M. Corticostriatal and corticosubthalamic input zones from the presupplementary motor area in the macaque monkey: comparison with the input zones from the supplementary motor area. Brain Res 1999;833: 191-201.

[18] Tachibana Y, Nambu A, Hatanaka N, Miyachi S, Takada M. Input–output organization of the rostral part of the dorsal premotor cortex, with special reference to its corticostriatal projection. Neurosci Res 2004;48: 45-57.

[19] Saga Y, Hirata Y, Takahara D, Inoue K, Miyachi S, Nambu A, Tanji J, Takada M, Hoshi E. Origins of multisynaptic projections from the basal ganglia to rostrocaudally distinct sectors of the dorsal premotor area in macaques. Eur J Neurosci 2011;33: 285-297.

[20] Hoshi E, Tanji J. Differential involvement of neurons in the dorsal and ventral premotor cortex during processing of visual signals for action planning. J Neurophysiol 2006;95: 3596-3616.

[21] Matelli M, Govoni P, Galletti C, Kutz DF, Luppino G. Superior area 6 afferents from the superior parietal lobule in the macaque monkey. J Comp Neurol 1998;402: 327-352.

[22] Luppino G, Rozzi S, Calzavara R, Matelli M. Prefrontal and agranular cingulate projections to the dorsal premotor areas F2 and F7 in the macaque monkey. Eur J Neurosci 2003;17: 559-578.

[23] Kaneda K, Nambu A, Tokuno H, Takada M. Differential processing patterns of motor information via striatopallidal and striatonigral projections. J Neurophysiol 2002;88: 1420-1432.

[24] Yelnik J, Percheron G, Francois C. A Golgi analysis of the primate globus pallidus. II. Quantitative morphology and spatial orientation of dendritic arborizations. J Comp Neurol 1984;227: 200-213.

[25] Yelnik J, Francois C, Percheron G, Heyner S. Golgi study of the primate substantia nigra. I. Quantitative morphology and typology of nigral neurons. J Comp Neurol 1987;265:455-472.

[26] Hazrati L-N, Parent A. Convergence of subthalamic and striatal efferents at pallidal level in primates: an anterograde double-labeling study with biocytin and PHA-L. Brain Res 1992;569: 336-340.

[27] Bolam JP, Hanley JJ, Booth PA, Bevan MD. Synaptic organisation of the basal ganglia. J Anat 2000;196 (Pt 4): 527-542.

[28] Parent A, Sato F, Wu Y, Gauthier J, Levesque M, Parent M. Organization of the basal ganglia: the importance of axonal collateralization. Trends Neurosci 2000;23: S20-27.

IntechOpen